XXII SITRAER 2025
Simpósio de Transporte Aéreo

AIR TRANSPORT NETWORK OPTIMIZATION APPLIED TO URBAN AIR MOBILITY OPERATIONS WITH AN EVTOL

Jose Alexandre Tavares Guerreiro Fregnani & Glaucia Costa Balvedi

Boeing Technology Innovation - Brazil

Corresponding author e-mail address: jose.a.fregnani@boeing.com

PAPER ID: SIT1217561

ABSTRACT

Urban Air Mobility (UAM) emerged as a disruptive concept, capable of driving new applications and services within the aerospace industry. This concept encompasses urban transportation systems that facilitate air travel for people, primarily addressing intracity passenger transport in response to traffic congestion, while offering competitive costs compared to terrestrial vehicles. The development of new vehicle designs, specifically electric Vertical Take-Off and Landing (eVTOL) aircraft has been pivotal in this evolution. According to predictions from the FAA and NASA, hundreds of eVTOLs are expected to share low-altitude airspace simultaneously in metropolitan environments within the next decade, marking a substantial shift in airspace and ground infrastructure operations. Unlike traditional commercial and regional aviation, urban air transport networks must be tailored to unique operational characteristics: low-altitude flights (up to 2000 ft), shorter distances (up to 100 km), flight durations (typically 10-15 minutes), ultra-fast turnaround times (up to 15 minutes), a significantly increased number of frequencies connecting network vertiports (up to 30 per day), and lower flight speeds (ranging from 80 to 150 kt). This paper proposes a method for computing the optimal network structure for a four-seater manned eVTOL operations on scheduled flights, based on a given daily passenger demand, while considering fixed speed-altitude and optimal flight profiles, with the objective of maximizing network profit. A case study involving a network of twelve vertiports in the São Paulo metropolitan area is analyzed. The results indicate that UAM can be economically viable in São Paulo if network and flight profile optimizations are effectively implemented. A key conclusion is that fully connected network use cases are not profitable, considering a ticket price of US$5,00 per km. Furthermore, relying solely on profile optimization is insufficient to ensure profitable operations and it was demonstrated that network optimization plays a critical role in enhancing profitability.

Keywords: Urban Air Mobility, Airline Network Optimization, Flight Operations, Aircraft Design, Multidisciplinary Design Optimization.

GENERATIVE AI USAGE STATEMENT

The authors declare that the use of generative AI tools was restricted to technical support activities, without compromising the originality, analysis, and conclusions presented in the work. All information obtained through these resources was carefully evaluated and integrated into the study, ensuring methodological rigor and academic integrity. Chat GPT was used to review the text.

PAPER ID: SIT1217561

AIR TRANSPORT NETWORK OPTIMIZATION APPLIED TO URBAN AIR MOBILITY OPERATIONS WITH AN EVTOL

1 INTRODUCTION

Urban Air Mobility (UAM), a subcategory of the Advanced Air Mobility (AAM) concept, represents a transformative innovation in urban transportation utilizing electric Vertical Take-Off and Landing (eVTOL) aircraft to provide rapid, low altitude intracity travels. Aimed at addressing the rising challenges of urban congestion and pollution, UAM offers a fast, sustainable alternative that could significantly enhance urban mobility.

As cities grow and population densities rise, UAM has the potential to reshape metropolitan transportation by reducing road congestion and decreasing travel times (NASA, 2020). Because of these potential benefits, UAM is being pursued in parallel with broader urban policy goals, most notably decarbonization, climate resilience, and equitable access to mobility, which shape how and where UAM will be deployed. Importantly, UAM development will not occur in isolation from concurrent urban planning and environmental movements. Cities worldwide are pursuing climate-resilient strategies that increase urban tree canopy, restore green spaces, and foster urban biodiversity to reduce heat, manage stormwater, and improve public health. These measures tend to increase the density and diversity of birdlife within metropolitan areas, including species known to pose bird strike risks to aircraft. At the same time, policies encouraging denser, mixed-use development and multimodal transport networks will influence demand patterns, vertiport siting, noise-sensitive land uses, and operational altitudes.

São Paulo, Brazil's largest metropolitan region and one of the world's ten most populous urban areas with approximately 22 million residents, serves as an ideal case study for UAM. The city already has a well-established helicopter network that supports 2200 flights daily operating at 260 helipads (DECEA, 2023) dedicated to business travel, medical emergencies, and cargo transport. This high demand makes São Paulo one of the busiest aerial corridors globally. However, despite the extensive use of helicopters, the city currently operates only two potential vertiports with infrastructure capable of supporting UAM, located in the districts of Osasco and Alphaville, in the west part of the city. Developing the necessary airport infrastructure and efficient transport networks will be essential to enable large-scale UAM profitable operations and fully explore the UAM market potential in São Paulo (O´Reilly et al., 2024).

The city's existing helicopter demand, limited vertiport infrastructure, and ongoing urban greening efforts together create both opportunity and complexity for UAM planning. Developing vertiport infrastructure and optimum eVTOL route networks, establishing safe low-altitude flight corridors, and integrating wildlife and environmental considerations will therefore be essential to enabling scalable and economically viable UAM operations while meeting urban sustainability goals.

1.1 OBJECTIVE

The primary objective of this research is to assess the economic viability of UAM operations in São Paulo metropolitan area. This will be developed by optimizing network and flight profiles using a single model of eVTOL operated by a fleet operator, connecting various vertiports within a designated portion of the metropolitan area. The optimization process aims to develop a model that maximizes profitability considering the passenger demand within the main regions of the city of Sao Paulo. By employing advanced computational modeling techniques, this research will identify the optimal network topology, flight paths, and energy consumption patterns. Ultimately, the goal is to determine the ideal number of flight frequencies and number of vehicles required to ensure efficient and profitable UAM operations.

2 LITERATURE REVIEW

The literature on UAM encompasses a diverse array of topics, including vehicle design, regulatory frameworks, infrastructure development, and network optimization. Both academic and industry research consistently underscore UAM's potential as a transformative urban transportation solution. Numerous studies delve into its technological, regulatory, and economic aspects to facilitate future implementation. Rapid advancements in electric propulsion and autonomous navigation have significantly accelerated UAM's development (Sunil et al., 2022). Key organizations, such as the Federal Aviation Administration (FAA) and the National Aeronautics and Space Administration (NASA), have been instrumental in advancing UAM by establishing foundational safety guidelines and promoting industry collaboration through initiatives like NASA's UAM Grand Challenge, which aims to expedite the development of essential UAM technologies (FAA, 2023).

A fundamental aspect of UAM is the progress in eVTOL technology, which enables vehicles to take off and land vertically using electric propulsion. This capability eliminates the need for extensive runways and reduces operational costs, thereby supporting more sustainable urban air transit solutions (Kim, 2023). Major aerospace companies, including Boeing, Airbus, and Embraer, have developed eVTOL prototypes that demonstrate the feasibility of UAM and its potential to revolutionize urban mobility considering the integration of the airspace with infrastructure (NASA, 2018). Designed for low-altitude operations, these vehicles provide a rapid and efficient alternative to ground-based transportation, particularly in congested urban areas. As urban airspaces become increasingly saturated, effective air traffic control and safety protocols are essential. Soykan, Ozerdem, & Baharozu (2017) explore the challenges of integrating eVTOLs with traditional aviation, while Abdellaoui et al. (2023) propose a layered airspace model that accommodates UAM routes while minimizing conflicts with existing aviation pathways.

The infrastructure for eVTOL operations is multifaceted, involving vertiports, air traffic management systems supported by cutting-edge communication, navigations and surveillance enablers, and robust energy supply networks. Brunelli, Ditta, & Postorino (2023) emphasize the importance of designing vertiports that prioritize accessibility, safety, and energy efficiency. Strategic placement and scalability are also crucial: Spirkovska et al. (2022) proposed models for integrating vertiports with urban transport hubs to enhance connectivity with other transit modes. Sunil et al. (2022) argue that seamless integration with ground transportation is vital for UAM's success. Furthermore, adequate charging infrastructure is necessary, although it remains limited in cities like São Paulo (FAA, 2023). As one of the largest global helicopter markets, São Paulo presents a unique opportunity for UAM, leveraging existing helicopter infrastructure to support initial eVTOL operations. However, additional vertiports and charging facilities are essential to scale up and meet the high demand for reliable, rapid transportation, particularly in the business and medical sectors (Brunelli, Ditta, & Postorino, 2023).

Sustainability is a key driver of UAM development, as eVTOLs offer significant environmental advantages over traditional helicopters. Operating on electricity, eVTOLs produce zero in-flight emissions and significantly reduce noise pollution, a critical consideration in urban environments (Uber elevate, 2016). Zhao et al. (2022) suggest that UAM's alignment with sustainability goals positions it as a valuable component of future urban transit systems. Despite these benefits, challenges remain, including regulatory hurdles, infrastructure demands, airspace integration, and public acceptance (Wang, Li, & Qu, 2023). Although eVTOLs generate less noise than traditional helicopters, noise remains a public concern. Studies indicate that public acceptance is crucial, as perceptions of safety and noise can influence adoption of this modal (Long et al., 2023). Onat et al. (2024) highlights the importance of regulatory adaptation and public engagement to address these issues. Similarly, Lopes & Silva (2023) examined public acceptance of UAM in São Paulo's metropolitan area, identifying key challenges and customer expectations that can inform public policies to enhance mobility in the region.

From an economic standpoint, UAM's profitability is essential for sustainable deployment in urban markets. Onat et al. (2024) and Straubinger & Fu (2029) emphasize the need for profitable models within the competitive urban transport sector. Jiang et al. (2024) analyze UAM's cost structure, including fixed operational, energy, and time-related expenses, providing a framework for effective pricing strategies. Additionally, Long et al. (2023) assess demand elasticity in response to ticket pricing, suggesting that strategic pricing can optimize revenue and maintain a stable passenger base, which is vital for financial viability.

Optimizing UAM networks is crucial for maximizing operational efficiency and economic performance, primarily through strategic route planning and frequency management. Genetic algorithms have shown promise in addressing complex optimization challenges, particularly in energy-sensitive applications like eVTOL flight profiles (Ha, Lee, & Hwang, 2019). Linear programming is another valuable tool for UAM network optimization, enabling fleet managers to balance route efficiency, demand, and operational costs (Papadimitriou & Steiglitz, 1982). Jaillet et al. (2015) emphasizes the importance of optimization algorithms for enhancing urban mobility networks, where route efficiency and reduced direct operational costs are essential for sustainability. Additionally, studies by Boo, Seung, & Song (2023) demonstrate that optimizing flight routes and schedules can significantly enhance efficiency and profitability. Techniques such as Mixed-Integer Linear Programming (MILP) are effective for route planning and fleet deployment in urban settings (van Schie et al., 2025). Fregnani, Mattos, & Hernandes (2019) propose an innovative approach to integrate aircraft design with network optimization within the same framework, considering the integration of a MILP problem embedded in a genetic algorithm to achieve simultaneous network and aircraft designs. This method involves comprehensive flight profile computation, considering the performance and operational aspects of commercial jetliners.

Beyond network routes, optimizing flight profiles is critical for minimizing energy consumption and maximizing range. Jang et al. (2021) demonstrate that refined climb, cruise, and descent profiles can reduce operational costs and improve battery performance. Given the high energy demands of eVTOLs, flight profile optimizations focused on cost-effectiveness and efficiency remain a priority for UAM providers.

The economic feasibility of eVTOL operations is closely tied to the cost per seat-kilometer, influenced by various operational factors. A comprehensive study (Goyal et al., 2021) analyzed nine eVTOL designs, revealing that a five-seat eVTOL could have an operating cost of approximately US$ 3,80 per seat-kilometer in the near term, lower than comparable services offered by helicopters, but higher than all surface transportation services. However, there are potential reductions down to US$ 1.3 per seat-kilometer as operational efficiencies and autonomous technologies advance. Other studies suggest that achieving profitability remains challenging. Furthermore, research indicates that battery-electric propulsion systems currently offer the lowest total cost of ownership for eVTOLs in sub-200 km applications, outperforming fuel cell and internal combustion engine alternatives, particularly as battery energy densities improve (Liu et al., 2023). Collectively, these studies underscore that while current eVTOL operational costs per seat-kilometer are higher than traditional ground transportation, ongoing technological advancements and strategic operational improvements are expected to enhance their economic feasibility in the future.

3 METHODOLOGY

A set of twelve node locations in São Paulo metropolitan area is selected from which the UAM network will be determined. These locations are chosen based on the proximity of the major business conglomerates areas from where busy traffic is well known in rush hours, existence of helipads (potential vertiports locations), and major metropolitan airports (Congonhas/CGH and São Paulo International/GRU). Table 1 shows the code-names and coordinates (latitude, longitude) of such locations. Figure 1 depicts the overview of the area of operations with all nodes- or potential vertiport locations - of the area considered.

Table 1: Network nodes (vertiports).

Name	Code	Longitude	Latitude
Congonhas	CGH	-46.6586	-23.6299
Morumbi	MORU	-46.6975	-23.6226
Faria Lima	LIMA	-46.6839	-23.6260
República	REPU	-46.6437	-23.5457
Guarulhos	GRU	-46.4812	-23.4396
Campo de Marte	MAE	-46.6393	-23.5116
Helicidade	HELI	-46.7375	-23.5471
Paulista	PAUL	-46.6522	-23.5642
Universiade Grande ABC	UABC	-46.5285	-23.6441
Centro Empresarial	CEMP	-46.6992	-23.6118
Ibirapuera	IBIR	-46.6569	-23.5851
Brooklin	EDIT	-46.6833	-23.6111

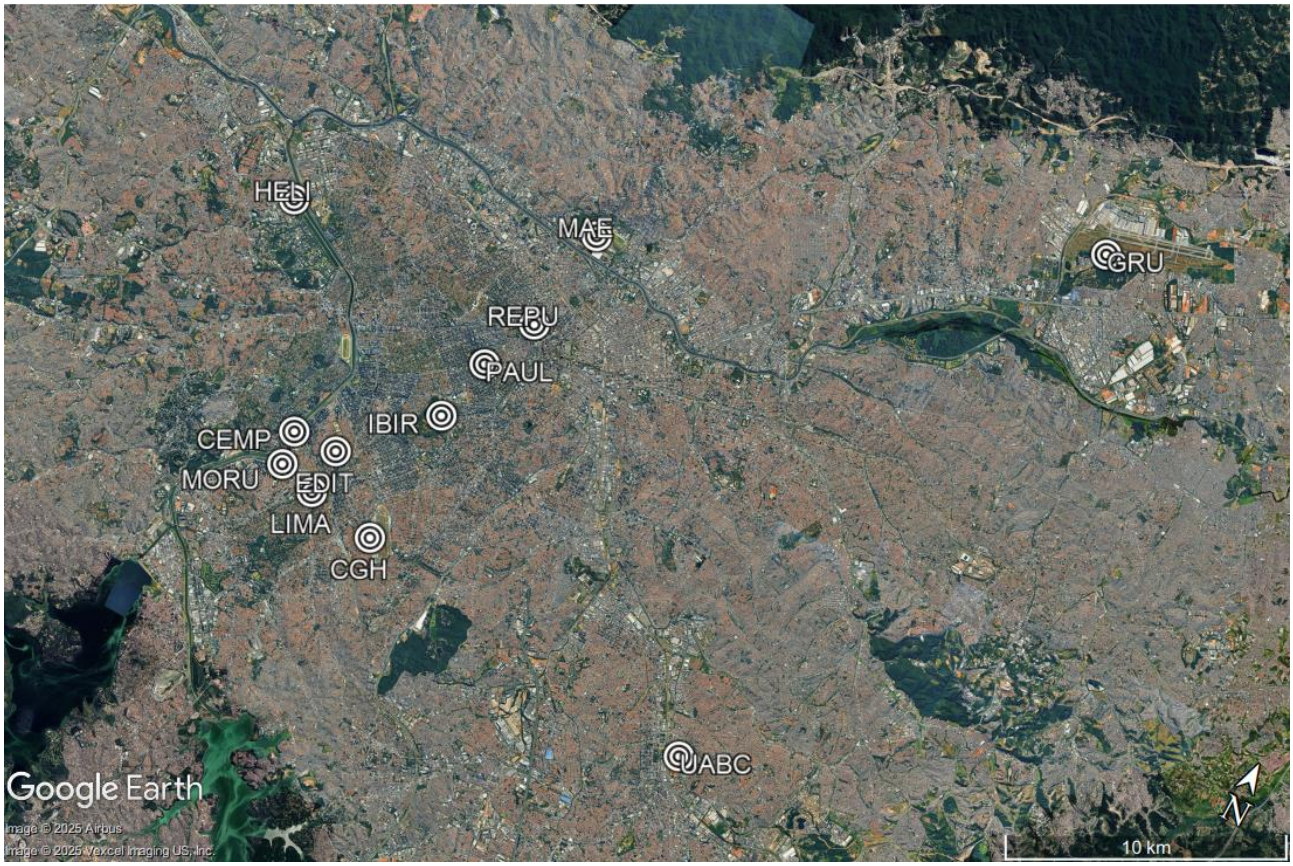

Figure 1: UAM network area of operations.

Daily passengers demand considered in this exercise is shown in Table 2. Demand values were determined based on the model proposed by Moita & Lopes (2016), considering car transport demand between zones in São Paulo metropolitan areas. It is assumed that eVTOLs would capture about 5% of car passenger demand between areas, in the first years of operations. The vehicle chosen for such operations is a generic piloted, tilted rotor eVTOL which characteristics are shown in Table 3. Figure 2 provides an illustrative example of this type of vehicle (European Union Safety Agency, 2022).

The optimization framework, illustrated in Figure 3, has been designed to identify the optimal network configuration and the appropriate number of frequencies for each connection, considering the operational characteristics of the selected vehicle. This framework aims to maximize the total network profit while meeting the specified passenger demands between vertiport pairs.

Additionally, it provides an estimate of the required fleet size, or the number of vehicles needed. To facilitate this process, a modular MATLAB® code has been developed.

Table 2: Estimated daily passengers demand between locations (number of passengers per day).

Origin	Destination											
	CGH	MORU	LIMA	REPU	GRU	MAE	HELI	PAUL	UABC	CEMP	IBIR	EDIT
CGH	0	37	33	32	29	33	37	33	32	29	29	29
MORU	37	0	37	33	32	29	33	37	33	32	29	29
LIMA	33	37	0	37	33	32	29	33	37	33	32	29
REPU	32	16	20	0	0	37	33	32	29	33	37	33
GRU	29	38	35	5	0	0	37	33	32	29	33	37
MAE	16	20	0	0	37	0	32	29	33	37	33	32
HELI	32	29	33	37	33	32	0	29	29	33	37	33
PAUL	32	16	33	37	33	0	37	0	32	29	33	37
UABC	29	38	29	33	37	33	0	37	0	32	29	33
CEMP	16	20	32	29	33	37	33	0	37	0	32	29
IBIR	32	29	37	37	33	33	37	33	37	33	0	29
EDIT	29	32	29	33	37	33	33	37	33	37	33	0

Table 3: Vehicle's operational characteristics.

Parameter	Value
Passengers Capacity	4
Piloted	Yes (1)
Design Cruise Speed	100 kt
Design Range	100 NM
Maximum Cruise Altitude	10000 ft
Maximum Takeoff Weight	2500 kg
Maximum Payload	500 kg
Maximum Remaining Battery Energy	40%
Batteries Energy Density	300 W.h/kg
Batteries Pack Weight	800 kg
Batteries Energy Full Capacity	150 KW.h

Figure 2: Example of eVTOL model (European Union Safety Agency, 2022).

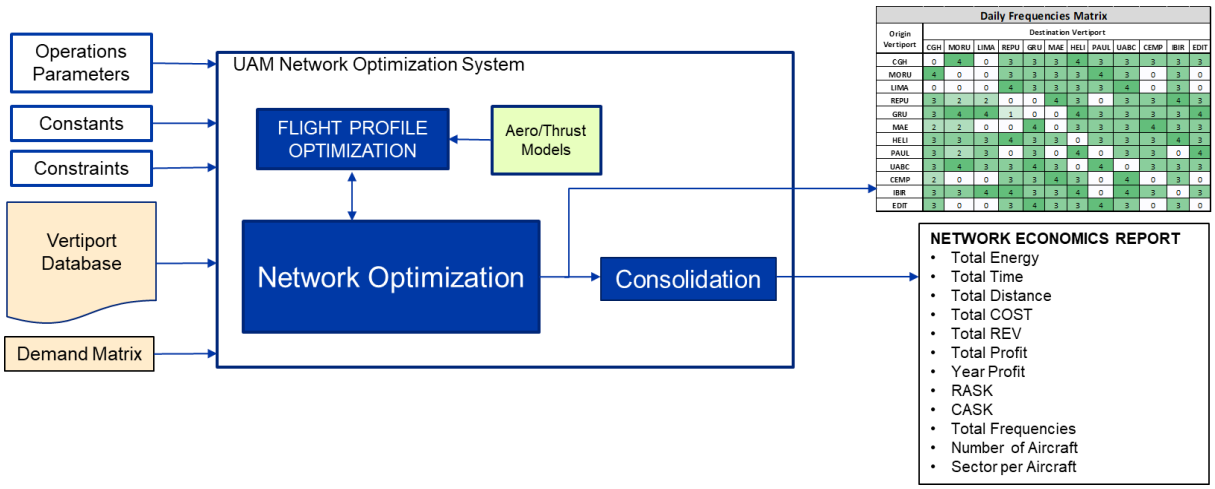

Figure 3: Network optimization framework.

The input parameters for the optimization module encompass the essential information utilized by the optimization processes. The Input Constants represent the numerical values of the vehicle's operational characteristics, as detailed in Table 3. Meanwhile, the Input Constraints define the upper and lower operational limits applied within the flight profile optimization module, which are outlined in Table 4.

Table 4: Input constraints.

Parameter	Range
Indicated Airspeed Speed	80 kt (1.3 Stall Speed) to 150 kt (Maximum Operational Speed)
Rate of Climb	- 2000 ft to +2000 ft per minute
Cruise Altitude	500 ft to 3000 ft above reference elevation

The Input Operations Parameters used in Network Optimization, as shown in Table 5, including the reference sources used to support the selected values. The vertiport database is loaded with the closest heliports information published by DECEA (2023) – assuming that the infrastructure of such heliports would be expanded to accommodate eVTOL operations. The types of each parameter in the Vertiports database are listed in Table 6.

Table 5: Input operations parameters.

Parameter	Acronym	Units	Value	Reference Source
Temperature Deviation from Standard Atmosphere	*ISADEV*	Deg C	10	Research assumptions
Average Load Factor	*LF*	%	75 (3 passengers)	
Average Grid Operator´s Energy Related Costs in Brazil (Vieira & Carpio, 2020)	C_e	US$/kW.h	0.20	(Vieira & Carpio, 2020)
Typical Fleet Operator´s Time Related Costs	C_t	US$/h	190.00	(Fiorti, Borghi, & Pavan, 2024)
Typical Fleet Operator´s Fixed Operations Cost	C_{fix}	US$	100.00	(Fiorti, Borghi, & Pavan, 2024)
Ticket Price per km	*p*	US$/km	5.00	Research assumptions
Energy Departure at each station	E_0	kW.h	150	
Vehicle Daily Utilization	*DU*	h	15	
Turn Around Time	*TAT*	min	15	

According to Fiorti et al. (2024), the composition of Direct Operating Costs for a representative four-seat eVTOL operation can be apportioned as follows: 19% capital (leasing), 19% crew, 9% energy, 4% fees (navigation and municipal), 26% maintenance, and 23% indirect operating costs (IOC, i.e., fixed overhead and infrastructure). These proportions are summarized in Figure 3. For the optimization presented here, time-dependent costs (*Ct*) include only the crew and maintenance components; capital, fees, and IOC are treated as fixed operating costs (*Cfix*) (see Table 5).

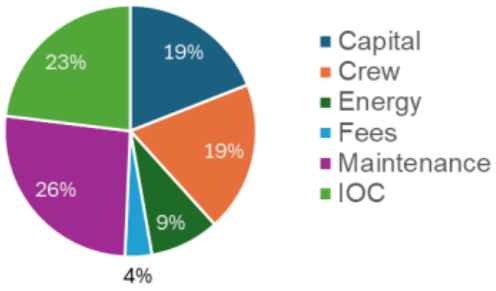

Figure 4: Typical Direct Operational Costs share for 4-seater eVTOLs (Fiorti, Borghi, & Pavan, 2024)

Table 6: Vertiport database.

Parameter	Type
Name	String
Code (5 letters)	String
Departure Latitude	Deg
Departure Longitude	Deg
Departure elevation	ft
Arrival Latitude	Deg
Arrival Longitude	Deg
Arrival elevation	ft

The flight profile optimization module calculates the optimal flight profile for each route, focusing on minimizing operational costs. To achieve this, it is essential to first assess the energy consumption and time required for the vehicle on each route. These parameters are determined through the development of lateral and vertical flight profiles, as explained below.

3.1 LATERAL FLIGHT PROFILE

The lateral flight profile is modeled as a great circle route between the origin (i) and destination (j) vertiports. Distances D_{ij} (in NM) between vertiports are determined via haversine formulae for loxodromic routes (Robusto, 1957).

3.2 VERTICAL FLIGHT PROFILE

The vertical flight profile is constructed according to flight phases, as illustrated in Figure 5. All altitudes are referred to as Mean Sea Level. The vehicle takes off and lands from the reference elevations of the respective departure and arrival vertiports ($elev_{dep}$ and $elev_{arr}$), in which arrival and departure temperatures area available (OAT_{dep} and OAT_{arr}) assumed to be obtained from local meteorological stations installed at each vertiport. In this simulation winds are considered calm.

The takeoff procedure involves a hover-out maneuver, after which the vehicle transitions to cruise speed using a tilt-down rotor technique. For simplicity, it is assumed that after takeoff this transition is completed at an altitude of 200 ft above the departure vertiport, taking approximately 2 minutes (T_{out}) and covering a distance of 1 NM from the origin (D_{out}). Similarly, during the approach and landing phases, the transition maneuver is assumed to begin at about 200 ft above the landing elevation, taking around 4 minutes (T_{in}) and covering a distance of 2.5 NM to decelerate from descent speed to hover-in (D_{in}). Along the vertical path outside of the transitions, the vehicle will climb, cruise, and descend at constant indicated air speeds: *CLBSPD*, *CRZSPD*, and *DESSPD*. Also, similar to a conventional general aviation aircraft, with a specified constant Rate of Climb (*RoC*), Rate of Descent (*RoD*), and Cruise Altitude (*CRZALT*). These parameters will serve as optimization variables

computed by the optimization algorithm.

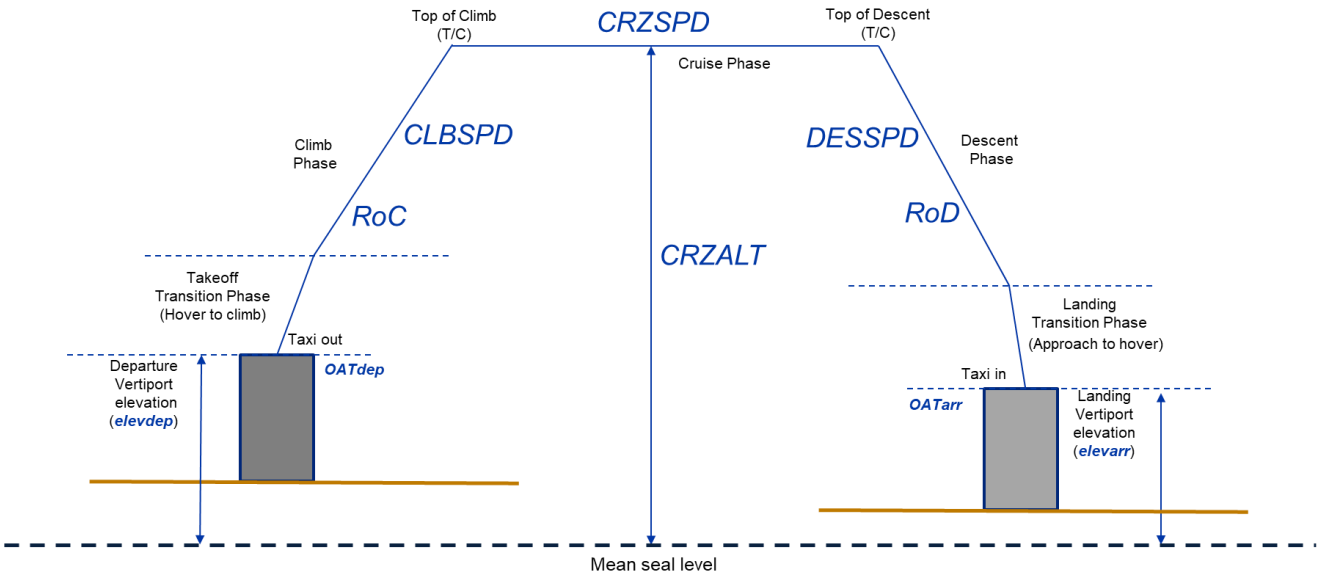

Figure 5: Vertical flight profile.

In all flight phases, it is assumed that the batteries pack can provide the required energy to sustain the flight considering the fixed operational variables. Since the operational speeds are expressed as indicated, they must be corrected to True Airspeeds along the flight segments (V_{clb}, V_{crz} and V_{des}) according to the following equations:

$$\sigma_{clb} = \left(\frac{(273.15 + ((OAT_{dep} + ISADEV - 0.00198 * ((\text{CRZALT} + \text{elev}_{dep})/2)}{288.15}\right)^{4.2288} \quad (1)$$

$$\sigma_{crz} = \left(\frac{(273.15 + ((OAT_{dep} + OAT_{arr})/2 + ISADEV - 0.00198 * \text{CRZALT})}{288.15}\right)^{4.2288} \quad (2)$$

$$\sigma_{des} = \left(\frac{(273.15 + (OAT_{arr} + ISADEV - 0.00198 * ((\text{CRZALT} + \text{elev}_{arr})/2)}{288.15}\right)^{4.2288} \quad (3)$$

$$V_{clb} = \frac{0.5144\ .\ CLBSPD}{\sqrt{\sigma_{clb}}}\ [\text{m/s}] \quad (4)$$

$$V_{crz} = \frac{0.5144\ .\ CRZSPD}{\sqrt{\sigma_{crz}}}\ [\text{m/s}] \quad (5)$$

$$V_{des} = \frac{0.5144\ .\ DESSPD}{\sqrt{\sigma_{des}}}\ [\text{m/s}] \quad (6)$$

The Total Profile Time (T_{tot}) is performed adding the time spent on each flight phase in addition to the hover-to-climb and approach-to-hover times (assumed T_h = 6 min). The following equations are applicable:

$$T_{tot} = T_h + T_{clb} + T_{des} + T_{crz}\ [\text{min}] \quad (7)$$

$$T_{clb} = 60.\frac{(CRZALT - Elev_{dep} - 200)}{RoC}\ [\text{min}] \quad (8)$$

$$T_{des} = 60.\frac{(CRZALT - Elev_{arr} - 200)}{RoD}\ [\text{min}] \quad (9)$$

$$T_{crz} = 3600.\frac{D_{crz}}{V_{crz}}\ [\text{min}] \quad (10)$$

Distances in climb, cruise and descent phases are calculated as follows:

$$D_{clb} = V_{clb} \ . T_{clb} + D_{out} \ \text{[NM]} \tag{11}$$

$$D_{des} = V_{des} . T_{des} + D_{in} \ \text{[NM]} \tag{12}$$

$$D_{crz} = D - D_{clb} - D_{des} \ \text{[NM]} \tag{13}$$

Where D is the total route distance.

The Total Profile Energy (E_{tot}) computation is performed adding the required energy in each flight phase in addition to the hover-to-climb and approach-to-hover energies (assumed E_h = 8 kW.h). The following equations are applicable:

$$E_{des} = 16.667 \, . \, 10^{-6} \, . \, T_{des} . \left(-W \, . \, g \, . \, 0.00508 \, . \, RoD + \left(\frac{1}{2} CD \, . \rho_0 \, . \, \sigma_{des} \, . \, S \, . \, {V_{des}}^3 \right) \right) \text{[kW.h]} \tag{14}$$

$$E_{crz} = 16.667 \, . \, 10^{-6} \, . T_{crz} \, . \, \left(\left(\left(\frac{CD}{CL} \right) . W \, . \, g \, . V_{crz} \right) \right) \text{[kW.h]} \tag{15}$$

$$E_{clb} = 16.667 \, . \, 10^{-6} \, . \, T_{clb} . \left(W \, . \, g \, . \, 0.00508 \, . \, RoC + \left(\frac{1}{2} CD \, . \, \rho_0 \, . \, \sigma_{clb} \, . \, S \, . {V_{clb}}^3 \right) \right) \text{[kW.h]} \tag{16}$$

$$E_{tot} = E_h + E_{des} + E_{crz} + E_{clb} \ \text{[kW.h]} \tag{17}$$

where ρ is the air density at the pressure altitude Hp, S is the reference area of the vehicle (in m^2), W is the weight of the vehicle (equal to MTOW) in kg, CL is the Lift Coefficient and g is the gravity constant (9.811 m/s^2). CD is the Drag Coefficient calculated via low-speed parabolic drag polar, defined according to the equations below:

$$CD = CD_0 + K . CL^2 \tag{18}$$

$$CL = \frac{2 . W}{\rho . S . V^2} \tag{19}$$

where V is the true air speed at the related phase of flight (V_{clb}, V_{des} or V_{crz}).

For the selected vehicle, the drag polar parameters are assumed to be CD_0 = 0.060 and K = 0.07. These values were chosen as multiples of parameters associated with a baseline general aviation aircraft, specifically the Piper PA28 Arrow (Johanson & Unell, 2014). The CD_0 value was derived using a factor of 2, indicating that the skin drag is twice that of the baseline aircraft. Similarly, the K value was determined using a factor of 1.3, suggesting that the vehicle would experience 30% more induced drag compared to the baseline. The authors consider these assumptions to be reasonable for low-speed aerodynamics in this type of eVTOL.

The remaining energy for the sector will be therefore:

$$E_{rem} = E_0 - E_{tot} \ \text{[kW.h]} \tag{20}$$

where E_0 is the Energy Departure at each station.

Finally, the Direct Operational Cost (C) associated with the profile is calculated as follows:

$$C = (C_{fix} + C_t . T_{tot} + C_e . E_{tot}) / D \ \text{[US\$/NM]} \tag{21}$$

where C_{fix} is the fleet operator´s fixed operations cost, C_t is the fleet operator´s time related costs, C_e the grid operator´s energy related costs and D the route distance.

3.3 FLIGHT PROFILE OPTIMIZATION

The flight profile as shown in Figure 5 may be optimized for minimum Direct Operational Cost (*C*), considering as design parameters the associated flight phase indicate air speeds (*CLBSPD*, *CRZSPD* and *DESSPD*), vertical speeds (*RoC* and *RoD*) and cruise altitude (*CRZALT*). This is done through the optimization cycle as shown in Figure 6, implemented in MATLAB®.

The vertical profile calculations are executed by the Flight Profile Computation Module. This module takes as input the operational parameters, constants, and design parameters (Xi). The output is the objective function (Fun), which represents the Direct Operational Cost (C) calculated for the associated flight profile.

In each iteration, the Optimization Algorithm Module adjusts the design parameters based on the Y input and feeds them back into the Flight Computation Module. The optimization process utilizes a Single Objective Genetic Algorithm (GA) function from the MATLAB® optimization package. Operational constraints are defined as upper and lower limits for the design variables within the function call. Specifically, VMIN = 50 kt and VMAX = 100 kt apply to CLBSPD, CRZSPD and DESSPD. For rate of climb limits, RoCMIN = -2000 ft/min and RoCMAX = +2000 ft/min are established.

The altitude constraints set the upper limit to 3000 ft above the reference altitude and the lower limit to 500 ft above the elevation of the origin or destination vertiports, whichever is higher. The convergence criteria for the GA algorithm are established based on either a 0.5% error in the computed consecutive objective function across iterations or a maximum of 1000 cycles, whichever occurs first. Before starting the network optimization process all possible flight routes shall be computed and assigned with their respective energy (E), time (T) and Direct Operational Cost (C).

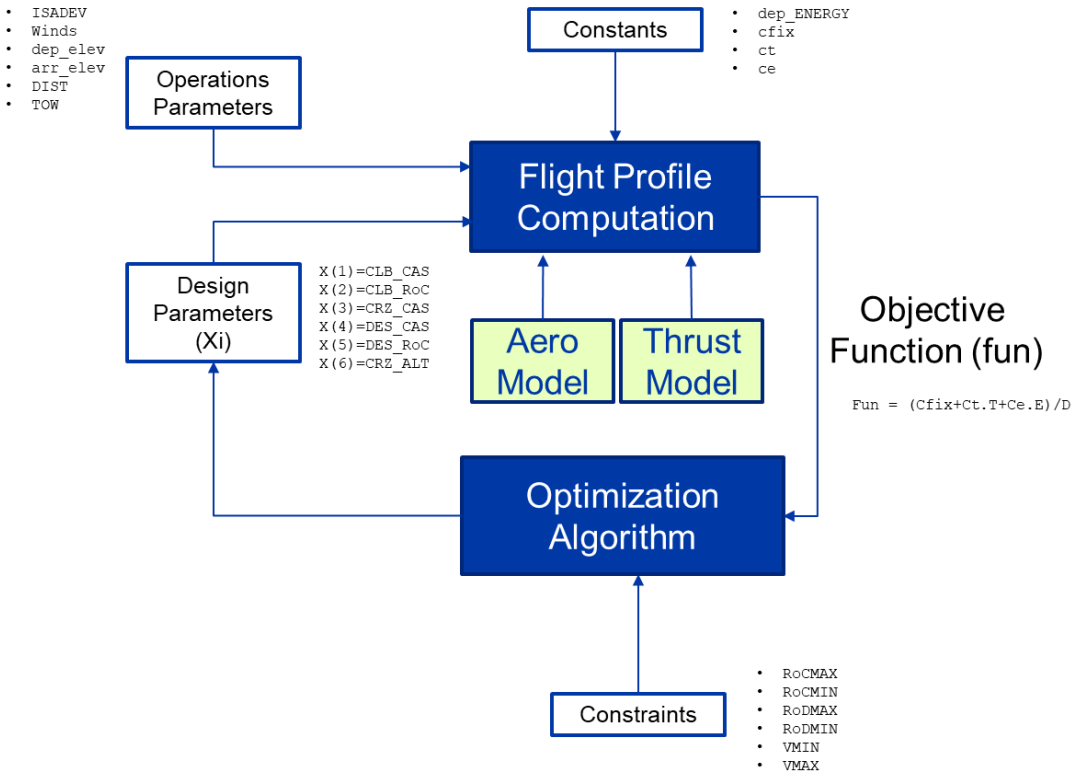

Figure 6: Flight profile optimization cycle.

3.4 NETWORK OPTIMIZATION

A MILP model is formulated for network optimization, aimed at maximizing profit by determining the optimal number of daily flights between vertiports. This framework does not account for aircraft allocation details such as tail assignment or scheduling for individual flight frequencies.

The optimization focuses on UAM networks operating within the city's defined geographical area. To develop an efficient network, essential parameters such as passenger demand between airports, average ticket prices, aircraft fleet capacity, range, and operational costs must be known. With this data, a profit-maximizing network can be designed. The profit is maximized when the entire potential passenger demand is satisfied for each city pair, with appropriate flight frequencies allocated for each aircraft type.

The model assumes that the UAM operator offers passengers the option to book flights with a maximum of two stops between their origin and destination. As a result, three types of services are considered: (i) non-stop flights, (ii) one-stop connecting flights, and (iii) two-stop connecting flights. Passenger ticket prices are modeled as a linear function of route distance, while operational costs are calculated based on energy consumption and travel time. In this research we assume a ticket price per distance flown (p) as 5.00 US$/km.

The optimization algorithm builds upon the Linear Programming Model (LPM) presented by Fregnani, Mattos, & Hernandes (2019), which addresses network design considering the fractional flow of passengers.

Let X_{iltj} be the fraction of the passenger's demand flow f_{ij} from origin i to destination j, served by a two-stop connecting flight through cities l and t, Y_{ij} the number of legs connecting i to j (route frequency), p the average ticket price per distance ($), C_{ij} the direct operational cost, b the passenger capacity of the vehicle, the reference load factor (LF) (assumed 75%) and D_{ij} the route distance between origin and destination vertiports. Given that, the following integer linear programming model is proposed:

$$\text{Maximize} \sum_{i \neq j} D_{ij}(b.LF.p - C_{ij}) \tag{22}$$

Subject to:

$$f_{ij} + \sum_{t \neq i,j}(f_{it}.X_{ijt} + f_{tj}.X_{tij} - f_{ij}.X_{itj}) + \sum_{i,t \neq i,j}(f_{lj}.X_{ltij} + f_{it}.X_{ijlt} - f_{ij}.X_{iltj}) \leq b.LF.Y_{ij} \tag{23}$$

for all i ≠ j

$$\sum_{t \neq i,j} X_{itj} + \sum_{l,t \neq i,j} X_{iltj} \leq 1 \tag{24}$$

for all i ≠ j

where X_{itj}, X_{iltj} are positive and Y_{ijk} integer positive for all $i \neq j$

The objective function (Equation 25) aims to maximize network profit. The constraint expressed by Equation 27 stipulates that the fractional flow on route ij must not exceed the total capacity of the assigned aircraft, while constraint expressed by Equation 28 ensures that the passenger flow for direct flights from i to j remains non-negative. It is assumed that 50% of the total passenger demand from i to j is generated by direct flights (X_{ij} and X_{ji}). Additionally, 30% of the demand is evenly distributed among all one-stop flights (X_{ijt}, X_{tij}, and X_{itj}), and 20% is evenly distributed among two-stop flights (X_{ltij}, X_{ijlt}, and X_{iltj}). The potential passenger demand between the origin and destination (f_{ij}) is sourced from Table 3. Figure 7 shows the graphical representation of the proposed network optimization model.

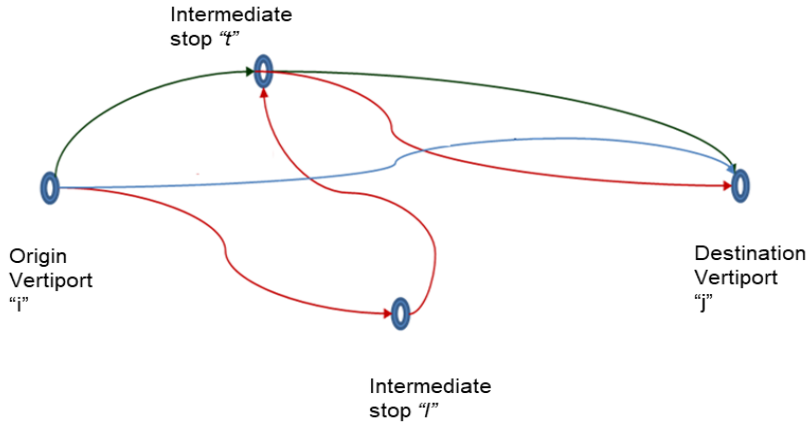

Xijt = fraction of demand captured from i to t with stop in j [%]
Xtij = fraction of demand captured from t to j with stop in i [%]
Xltij = fraction of demand captured from l to j with stops in t and i [%]
Xiltj = fraction of demand captured from i to j with stops in l and t [%]
fij = demand between vertiports i and j
ftj = demand between vertiports t and j
flj = demand between vertiports l and j
fit = demand between vertiports i and t

Figure 7: Network optimization model (Fregnani, Mattos, & Hernandes, 2019).

3.5 CONSOLIDATION MODULE

In this module the results related to economics of the transport network are consolidated. Total Network Profit (*NP*), Revenue (*NR*), Costs (*NC*) and Profit Margin (*PM*) are computed according to Equations 29 to 32, as function of route frequency Y_{ij}, route distance D_{ij}, aircraft passenger capacity b, average load factor (*LF*), sector Direct Operational Cost (C_{ij}) and average ticket price per distance (p) as follows:

$$NC = \sum_{i=1}^{N}\sum_{j=1}^{N}(C_{ij}.Y_{ij}.D_{ij}) \, , for \; i \neq j \tag{25}$$

$$NR = \sum_{i=1}^{N}\sum_{j=1}^{N}(p.b.LF.Y_{ij}.D_{ij}) \, , for \; i \neq j \tag{26}$$

$$NP = NR - NC \tag{27}$$

$$M = 100 * \left(\frac{NR}{NC} - 1\right) \tag{28}$$

In addition, the estimated fleet size (N) for the associated network is calculated according to Equation 33, as function of average daily utilization (*DU*), sector flight time (T_{ij}) and average turnaround time (*TAT*) as follows:

$$N = int\left(\frac{\sum_{i=1}^{N}\sum_{j=1}^{N}(T_{ij} + TAT)}{DU}\right), for \; i \neq j \tag{29}$$

4 RESULTS AND ANALYSIS

Given the proposed framework, three optimized scenarios (Sections 5.2, 5.3, and 5.4) were simulated and compared with a baseline scenario (Section 5.1) in which the network is fully connected. Results and their analysis are described below.

4.1 FIXED NETWORK WITH FIXED FLIGHT PROFILE (BASELINE SCENARIO)

The baseline scenario is the one where all vertiports of the network are fully connected and represent the first attempt of operators to get maximum profit without any optimization. Flight profiles are constructed considering fixed speed parameters, as usual in short urban helicopter operations, defined as follows:

- Cruise Altitude: 1000 ft above average elevation between vertiports
- Climb Speed: 85 kt (indicated airspeed)
- Cruise Speed:100 kt (indicated airspeed)
- Descent Speed: 95 kt (indicated airspeed)
- Operational parameters are listed in Tables 5 and 6

Table 7 presents the daily frequency matrix, detailing the necessary frequencies to meet demand. Notably, the vertiport with the highest accumulated frequencies is IBIR, indicating its potential as a central hub within the network.

Table 7: Daily frequencies matrix - baseline scenario.

Origin	**Destination**											
	CGH	MORU	LIMA	REPU	GRU	MAE	HELI	PAUL	UABC	CEMP	IBIR	EDIT
CGH	0	4	3	3	3	3	4	3	3	3	3	3
MORU	4	0	4	3	3	3	3	4	3	3	3	3
LIMA	3	4	0	4	3	3	3	3	4	3	3	3
REPU	3	2	2	0	0	4	3	3	3	3	4	3
GRU	3	4	4	1	0	0	4	3	3	3	3	4
MAE	2	2	0	0	4	0	3	3	3	4	3	3
HELI	3	3	3	4	3	3	0	3	3	3	4	3
PAUL	3	2	3	4	3	0	4	0	3	3	3	4
UABC	3	4	3	3	4	3	0	4	0	3	3	3
CEMP	2	2	3	3	3	4	3	0	4	0	3	3
IBIR	3	3	4	4	3	3	4	3	4	3	0	3
EDIT	3	3	3	3	4	3	3	4	3	4	3	0

Table 8 presents the yearly performance results of the network's economics. It is important to note that this scenario resulted in an annual loss of $3.25 million, reflecting a profit margin of -12.5% with a fleet of 11 vehicles. This outcome underscores the necessity for optimization—both in network design and flight profiles—to achieve economic viability at a ticket price of $5.00 per kilometer. To make operations profitable under this network topology, the ticket price would need to be increased to $5.43 per kilometer, assuming the same number of passengers is transported.

Table 8: Network economics - baseline scenario.

Parameter	**Units**	**Value**
Total Energy	kW.h	6857.6
Total Time	Min	2391
Power Required	MW	0.17
Toal Distance	NM	2562.1
Total PAX	-	1197
Total Daily Cost	US$	$ 80092.23
Total Daily Revenue	US$	$ 71175.14
Total Daily Profit	US$	($ 8917.09)
Year Profit	Millions of US$	($ 3.25)
Profit Margin	%	-12.53
Total Number of Frequencies	-	399
Number of Vehicles Required	-	11
Sectors per Aircraft	-	36

4.2 FIXED NETWORK WITH OPTIMIZED FLIGHT PROFILE

In this scenario, all vertiports remain interconnected within the network, while flight profiles are optimized based on the specified design variables (*CLBSPD*, *CRZSPD*, *CRZALT*, *DESSPD*, *RoC*, and *RoD*), adhering to their respective limits. The operational parameters utilized in the simulation are detailed in Tables 6(a, b).

Table 9 presents the required frequencies to meet the demand, illustrated in a daily frequency matrix. Notably, the vertiport with the highest accumulated frequencies is HELI, indicating its potential as a central hub within the network. It is important to note that some route connections were excluded due to non-converging optimal solutions, as determined by the constraints of the genetic algorithm (GA).

In all valid sectors, the climb speed was chosen to be close to the maximum rate of climb speed of 95 kt (*RoC* of 1500 ft/min), the cruise speed approached the maximum operating speed of 150 kt, and the descent speed was set near the maximum lift-to-drag ratio speed of 96 kt (*RoD* of - 500 ft/min). The scheduled cruise altitude varied from 500 ft to 2700 ft above the average elevations of the origin and destination vertiports. Additionally, it was observed that longer sectors corresponded to higher selected cruise altitudes. For the longest sector (GRU-CEMP / 30.9 km), the cruise altitude was established at 2700 ft above the average vertiport elevation. Figure 8 (Appendix) illustrates the map view of all route connections.

Table 10 displays the yearly performance results of the network's economics, along with a comparison (deltas) to the baseline scenario. It is noteworthy that this scenario still resulted in an annual loss of $0.92 million, which corresponds to a profit margin of -3.65%. This marks a 76% improvement compared to the baseline scenario, utilizing a fleet of 8 vehicles. This outcome further emphasizes the necessity for comprehensive network optimization—not just profile adjustments—to achieve economic viability at a ticket price of $5.00 per kilometer. To render operations profitable under this network topology, the ticket price would need to be increased to $5.18 per kilometer, assuming the same number of passengers is transported.

Table 9: Daily frequencies matrix for the Fixed Network/Optimum Flight profile scenario.

Origin	Destination											
	CGH	MORU	LIMA	REPU	GRU	MAE	HELI	PAUL	UABC	CEMP	IBIR	EDIT
CGH	0	4	0	3	3	3	4	3	3	3	3	3
MORU	4	0	0	3	3	3	3	4	3	0	3	0
LIMA	0	0	0	4	3	3	3	3	4	0	3	0
REPU	3	2	2	0	0	4	3	0	3	3	4	3
GRU	3	4	4	1	0	0	4	3	3	3	3	4
MAE	2	2	0	0	4	0	3	3	3	4	3	3
HELI	3	3	3	4	3	3	0	3	3	4	3	3
PAUL	3	2	3	0	3	0	4	0	3	3	0	4
UABC	3	4	3	3	4	3	0	4	0	3	3	3
CEMP	2	0	0	3	3	4	3	0	4	0	3	0
IBIR	3	3	4	4	3	3	4	0	4	3	0	3
EDIT	3	0	0	3	4	3	3	4	3	0	3	0

Table 10: Network economics - Fixed Network/Optimum Flight profile scenario.

Parameter	Units	Use Case Values	Baseline Values	Difference Values	Difference %
Total Energy	kW.h	4081.5	6857.6	-2776.1	-40.5%
Total Time	Min	1222	2391	-1169	-48.9%
Power Required	MW	0.20	0.17	0.03	17.6%
Toal Distance	NM	2501.3	2562.1	-60.8	-2.4%
Total PAX	-	1026	1197	-171	-14.3%
Total Daily Cost	US$	$ 72018.21	$ 80092.23	($8074.02)	-10.1%
Toal Daily Revenue	US$	$ 69484.90	$ 71175.14	($1690.24)	-2.4%
Total Daily Profit	US$	($2533.31)	($8917.09)	$6383.78	71.6%
Year Profit	Millions of US$	($0.92)	($3.25)	$2.33	71.6%
Profit Margin	%	-3.65	-12.53	8.88	70.9%
Total Number of Frequencies	-	342	399	-57	-14.3%
Number of Vehicles Required	-	8	11	-3	-27.3%
Sectors per Aircraft	-	43	36	7	19.4%

4.3 OPTIMIZED NETWORK WITH FIXED FLIGHT PROFILE

In this scenario, network optimization is performed to determine the route frequencies and fleet size that maximize the total profit for the assigned demand field, however considering the fixed flight profile from the baseline case. Table 11 shows all necessary frequencies to fulfill the demand (daily frequencies matrix). It might be noticed that the vertiport which provides more frequencies accumulated is GRU and therefore may represent a potential hub for such network. It may be noticed that this vertiport is the one that provides longer route distances and therefore the one which profit is mostly influenced by the ticked price per passenger (which is a function of distance). It should be noticed that most of the routes not originating from GRU were removed, due to non-profitable solutions.

In Table 12 the network economics yearly performance results and comparison (deltas) with baseline scenario are shown. It shall be noticed that this scenario finally resulted in an annual profit of 0.52 million US$, representing a profit margin of 6.23% (improvement of 149.7% when compared with the baseline) and considering a 2 vehicles fleet. This result highlights the benefits of the network optimization to achieve economic viability if the ticked price is charged at 5.00 US$/km level, even removing some sectors. In this case, the breakeven ticket price would be 4.81 US$/km if considering the same number of passengers transported.

Table 11: Daily Frequencies matrix for the Optimum Network/Fixed Flight profile.

Origin	**Destination**											
	CGH	MORU	LIMA	REPU	GRU	MAE	HELI	PAUL	UABC	CEMP	IBIR	EDIT
CGH	0	0	0	0	3	0	0	0	0	0	0	0
MORU	0	0	0	0	3	0	0	0	0	0	0	0
LIMA	0	0	0	0	3	0	0	0	0	0	0	0
REPU	0	0	0	0	0	0	0	0	0	0	0	0
GRU	3	4	4	1	0	0	4	3	3	3	3	4
MAE	0	0	0	0	4	0	0	0	0	0	0	0
HELI	0	0	0	0	3	0	0	0	3	0	0	0
PAUL	0	0	0	0	3	0	0	0	0	0	0	0
UABC	0	0	0	0	4	0	0	0	0	0	0	0
CEMP	0	0	0	0	3	0	0	0	0	0	0	0
IBIR	0	0	0	0	3	0	0	0	0	0	0	0
EDIT	0	0	0	0	4	0	0	0	0	0	0	0

Table 12: Network economics - Optimum Network/ Fixed Flight profile scenario.

Parameter	**Units**	**Use Case Values**	**Baseline Values**	**Difference Values**	**%**
Total Energy	kW.h	2212.1	6857.6	4645.5	-67.7%
Total Time	Min	691	2391	1700	-71.1%
Power Required	MW	0.18	0.17	0.01	5.9%
Toal Distance	NM	938.54	2562.1	-1623.6	-63.4%
Total PAX	-	189	1197	-1008	-84.2%
Total Daily Cost	US$	$ 24447.94	$ 80092.23	($55644.29)	-69.5%
Toal Daily Revenue	US$	$ 26072.57	$ 71175.14	($45102.57)	-63.4%
Total Daily Profit	US$	$1624.63	($8917.09)	$10541.72	118.2%
Year Profit	Millions of US$	$0.59	($3.25)	$3.85	118.2%
Profit Margin	%	6.23	-12.53	18.76	149.7%
Total Number of Frequencies	-	63	399	-336	-84.2%
Number of Vehicles Required	-	2	11	-9	-81.8%
Sectors per Aircraft	-	32	36	-4	-11.1%

4.4 OPTIMIZED NETWORK WITH OPTIMIZED FLIGHT PROFILE

In this scenario, both network and profile optimization are conducted to determine route frequencies and fleet size that maximize total profit for the assigned demand field.

Table 13 presents the daily frequency matrix, outlining the necessary frequencies to meet demand. Notably, the vertiport with the highest accumulated frequencies is once again GRU, indicating its potential as a central hub within the network. Like the previous simulation, it is evident that GRU offers the longest route distances, making its profitability significantly influenced by the ticket price

per passenger, which is a function of distance. It is important to note that most routes not originating from GRU were removed due to non-profitable solutions, as well as those for which the profile could not achieve an optimal solution. Additionally, the optimization revealed another potential hub at UABC.

As observed previously, in all valid sectors, the climb speed was selected to be close to the maximum rate of climb speed of 95 kt (*RoC* of 1500 ft/min), the cruise speed approached the maximum operating speed of 150 kt, and the descent speed was set near the maximum lift-to-drag ratio speed of 96 kt (*RoD* of -500 ft/min). The scheduled cruise altitude varied from 600 ft to 2800 ft above the average elevations of the origin and destination vertiports. It was noted that longer sectors corresponded to higher selected cruise altitudes. Table 14 presents the yearly performance results of the network's economics, along with a comparison (deltas) to the baseline scenario. Notably, this scenario achieved the highest annual profit of $5.2 million, reflecting a profit margin of 34.3%, which represents a remarkable improvement of 374.1% compared to the baseline, utilizing a fleet of 3 vehicles. This outcome underscores the advantages of network optimization in achieving economic viability, even with the removal of certain sectors, at a ticket price of $5.00 per kilometer. In this scenario, the breakeven ticket price would be $3.25 per kilometer, assuming the same number of passengers is transported. Finally, a summary of the results from all four simulations are shown in Table 15.

Table 13: Daily Frequencies matrix for the Optimum Network/Optimum Flight profile.

Origin	Destination											
	CGH	MORU	LIMA	REPU	GRU	MAE	HELI	PAUL	UABC	CEMP	IBIR	EDIT
CGH	0	0	0	0	3	0	0	0	0	0	0	0
MORU	0	0	0	0	3	3	0	0	3	0	0	0
LIMA	0	0	0	0	3	0	0	0	4	0	0	0
REPU	0	0	0	0	0	0	0	0	3	0	0	0
GRU	3	4	3	1	0	0	4	3	3	3	3	4
MAE	0	2	0	0	4	0	0	0	3	0	0	0
HELI	0	0	0	0	3	0	0	0	3	0	0	0
PAUL	0	0	0	0	3	0	0	0	3	0	0	0
UABC	0	4	3	3	4	3	0	4	0	3	3	3
CEMP	0	0	0	0	3	0	0	0	4	0	0	0
IBIR	0	0	0	0	3	0	0	0	4	0	0	0
EDIT	0	0	0	0	4	0	0	0	3	0	0	0

Table 14: Network economics - Optimum Network/ Optimum Flight profile scenario.

Parameter	Units	Use Case Values	Baseline Values	Difference Values	Difference %
Total Energy	kW.h	2450.3	6857.6	-4407.3	-64.3%
Total Time	Min	570	2391	1821	-76.2%
Power Required	MW	0.26	0.17	0.09	52.9%
Toal Distance	NM	1502.2	2562.1	-1059.9	-41.4%
Total PAX	-	375	1197	-822	-68.7%
Total Daily Cost	US$	$27400.00	$ 80092.23	($52692.04)	-65.8%
Toal Daily Revenue	US$	$41730.87	$ 71175.14	($29444.27)	-41.4%
Total Daily Profit	US$	$14330.68	($8917.09)	($23444.27)	260.7%
Year Profit	Millions of US$	5.23	($3.25)	8.49	260.7%
Profit Margin	%	34.34	-12.53	46.87	374.1%
Total Number of Frequencies	-	124	399	-275	-68.9%
Number of Vehicles Required	-	3	11	-8	-72.7%
Sectors per Aircraft	-	42	36	6	16.7%

Table 15: Summary of network/profile simulations.

	Fixed Network Fixed Profile (Baseline)	Fixed Network Optimum Profile	Optimum Network Fixed Profile	Optimum Network Optimum Profile
Number of connections	125	107	20	39
Number of vehicles	11	8	2	3
Year Profit (Mi US$)	-3.255	-0.925	0.593	5.231
Profit Margin (%)	-12.5%	-3.7%	6.2%	34.3%
Break Even ticket price (US$/km)	5.43	5.18	4.81	3.25

5 CONCLUSIONS

The results of this study indicate that Urban Air Mobility (UAM) operations in São Paulo can be economically viable, but viability is contingent on rigorous network design and coordinated operational strategy. This research analysis shows that a fully connected network operating at the baseline fare of USD 5.00 per kilometer is not financially sustainable. Conversely, network optimization — including selective vertiport placement, route consolidation, and demand-responsive scheduling — plays a decisive role in improving unit economics; flight-profile refinements alone are insufficient to secure profitability. Under a scenario combining an optimized network with optimized flight profiles, the model suggests that fares could be reduced to approximately USD 3.25 per kilometer while maintaining positive financial performance, which would make UAM more competitive with ground alternatives.

Despite these encouraging results, several material uncertainties temper the conclusions. First, projected passenger demand and modal shift behavior are sensitive to assumptions about price elasticity, travel-time savings, service frequency, and customer segmentation; empirical demand estimates are required to validate modeled uptake. Second, large-scale deployment will depend on the availability and cost of supporting infrastructure — additional vertiports, charging stations, and ground access facilities — and on the timeline and expense of their development. Third, environmental and operational risks associated with urban greening (increased bird abundance) and other wildlife dynamics introduce potential safety and reliability challenges that must be quantified and mitigated. Fourth, regulatory evolution — including airspace integration, certification pathways, and noise standards — will shape allowable operations and cost structures. Finally, technological trajectories for vehicle certification, autonomy, noise reduction, and battery performance will materially affect operating costs and service capability.

Given the nonlinear interactions among these factors, projections reported here should be interpreted as conditional and scenario-dependent. Future research priorities include empirical demand studies under varied pricing and service scenarios; comprehensive cost assessments for vertiport and charging infrastructure; wildlife hazard analyses in greening urban environments and evaluations of avian detection/avoidance systems; assessments of community acceptance and noise mitigation strategies; and scenario modeling that couples regulatory, technological, and environmental uncertainties. Proactive coordination among operators, planners, regulators, and communities will be essential to reconcile UAM deployment with São Paulo's broader sustainability and mobility objectives, and to position the city as a replicable model for responsible UAM implementation.

6 REFERENCES

Abdellaoui, R., Naser, R., Stasika, I., Hagag, N., Lee, H., & Moolchandani, K. (2023). Building a Performance Comparison Framework for Urban Air Mobility Airspace Management Concepts. *IEEE/AIAA 42nd Digital Avionics Systems Conference (DASC).*

Boo, J., Seung, Y., & Song, B. (2023). The UAM service network: multi-objective and multi-period design for UAM airports. *Asia Pacific Journal of Marketing and Logistics*.

Brunelli, M., Ditta, C., & Postorino, M. (2023). New infrastructures for Urban Air Mobility systems: A systematic review on vertiport location and capacity. *Journal of Air Transport Management*.

DECEA. (2023). *Anuário Estatístico de Tráfego Aéreo.* Rio de Janeior: Departamento de Controle do Espaço Aéreo.

European Union Safety Agency. (2022). *Prototype Technical Specifications for the Design of VRF Vertiports fo Operation with Manned VTOL-Capable Aircraft Certified in the Enhanced Cathegory.* EASA.

FAA. (2023). *UAM Concept of Operations 2.0.* Washinghton D.C. (USA): Federal Aviation Admisnistration .

Fiorti, M., Borghi, M., & Pavan, G. (2024). Environmental and economic assessment of an eVTOL aircraft fleet for Urban Air Mobility. *ICAS.* Florence.

Fregnani, J., Mattos, B., & Hernandes, J. (2019). Multidisciplinary and multi-objective optimization considering aircraft program cost and airline network. *Journal of Air Transportation*, p. 29.

Goyal, R., Reiche, C., Fernando, C., & Cohen, A. (2021). Advanced air mobility: Demand analysis and market potential of the airport shuttle and air taxi markets. *Suatainability*, pp. v. 13, n. 13, p. 7421.

Ha, T., Lee, K., & Hwang, J. (2019). Large-scale design and economics optimization of eVTOL concepts for urban air mobility. *AIAA Scitech 2019 Forum* .

Jaillet, P., Qi, J., & Sim, M. (2015). Routing Optimization Under Uncertainty. *Operations Research*.

Jiang, X., Cao, S., Mo, B., Cao, j., Yang, H., Tiang, Y., & Sengupta, R. (2024). Simulation-Based Optimization for Vertiport Location Selection: A Surrogate Model With Machine Learning Method. *Transportation Research Record*.

Johanson, E., & Unell, F. (2014). *Flight Testing of the Piper PA-28 Cherokee Archer II Aircraft.* KTH.

Kim. (2023). Electric Propulsion in Urban Air Mobility. *Aeronautics Quaterly*.

Liu, M., Hao, H., Lin, Z., He, X., Qian, Y., Sun, X., . . . Zao, F. (2023). Flying cars economically favor battery electric over fuel cell and internal combustion engine. *PNAS nexus*, p. pgad019.

Long, Q., Ma, J., Jiang, F., & Webster, C. (2023). Demand analysis in urban air mobility: A literature review. *Journal of Air Transport Management*.

Lopes, D., & Silva, J. (2023). Urban air mobility (UAM) in the metropolitan region of São Paulo: Potential and threats. *Journal of Airline and Airport Management*, pp. 1-11.

Moita, R., & Lopes, D. (2016). Demanda por meios de transporte na grande São Paulo: uma análise de políticas públicas. *Pesquisa e Planejamento Econômico*, pp. 125-149.

Moritz, H. (1980). Geodetic Reference System . *Bulletin Géodésique*, pp. 395-405.

NASA. (2018). *Urban Air Mobility Airspace Integration Concepts and Considerations.* Wshington D.C. (USA): National Aeronautics and Space Administration.

NASA. (2020). *Urban Air Mobility Overview.* Washington D.C. (USA): National Aeronautics and Space Administration.

O´Reilly, P., Rahimi, R., Marques, J., & Babadopoulos, M. (2024, July). Vertiport ventures: assessing operational feasibility for eVTOL integration in São Paulo's helipad and heliport infrastructure. *Journal of Marketing Analytics*.

Onat, B., Bulusu, V., Chakrabarty, A., Hansen, M., Sengupta, R., & Sridhar, B. (2024). Evaluating eVTOL Network Performance and Fleet Dynamics through Simulation-Based Analysis. *In AIAA SCITECH 2024 Forum.*

Papadimitriou, C., & Steiglitz, K. (1982). *Combinatorial optimization: algorithms and complexity.* Englewood Cliffs (USA): Prentice Hall.

Robusto, C. C. (1957). The cosine-harvesine formula. *The Americal Mathematical Monthly, 64*(1), 30-40.

Soykan, G., Ozerdem, M., & Baharozu, E. (2017). Future aircraft concept in terms of energy efficiency and environmental factors. *Energy*, pp. 1368-1377.

Spirkovska, L., Kulkami, S., Watkins, J., & MARtin, L. (2022). Urban air mobility airspace dynamic density. *AIAA Aviation 2022 Forum.*

Straubinger, A., & Fu, M. (2029). Identification of strategies how urban air mobility can improve existing public transport networks. *Mobil TUM.* Munich (Germany).

Sunil, E., Hoekstra, J., Elenbroek, J., Bassink, F., Nieuwenhuisen, D., Vidosavljevic, A., & Kern, s. (2022). Relating airspace structure and capacity for extreme traffic densities. *USA/EUROPE ATM 2015 Seminar.*

Uber elevate. (2016). *Fast-Forwarding to a Future of an On-Demand Urban Air Transportation.* UBER.

van Schie, S., Fletcher, H., Warner, M., Sperry, M., Scotzniovsky, L., & Hwang, T. (2025). Large-Scale Distributed Multidisciplinary Design Optimization of the NASA Lift-Plus-Cruise Air Taxi Concept. *AIAA SCITECH 2025 Forum.*

Vieira, S., & Carpio, L. (2020). The economic impact on residential fees associated with the expansion of grid-connected solar photovoltaic generators in Brazil. *Renewable Energy*, pp. 1084-1098.

Wang, K., Li, A., & Qu, X. (2023). Urban aerial mobility: Network structure, transportation benefits, and Sino-US comparison. *The Innovation*.

Yang, C., Liu, T., Ge, S., Rountree, E., & Wang, C. (2021). Challenges and key requirements of batteries for electric vertical takeoff and landing aircraft. *Joule*.

Zhao, P., Post, J., Wu, Z., Du, W., & Zhang, Y. (2022). Environmental impact analysis of on-demand urban air mobility: A case study of the Tampa Bay Area. *Transportation Research Part D: Transport and Environment*.